Bull. Fish. Sci. Hokkaido Univ.
74(1), 23-33, 2024.
DOI 10.14943/bull.fish.74.1.23

East-west differences of the microplankton community along the 47°N transect in the subarctic Pacific during the summer of 2021

Kosuke EGASHIRA[1)]*, Yu-Sin HUANG[2)], Kohei MATSUNO[3),4)] and Atsushi YAMAGUCHI[3),4)]

(Received 12 February 2024, Accepted 8 April 2024)

Abstract

The subarctic Pacific includes the coast of Hokkaido in the west to the Gulf of Alaska in the east. This region is known as one of the worlds major high nutrient low chlorophyll ocean areas. Despite its importance, little information is available about the east-west differences in the microplankton communities of this region. This study examined east-west differences in the microplankton community structure along the transect of 47°N latitude in the subarctic Pacific during July-August 2021. The microplankton cell density at each station ranged between 2.3 and 117.8 cells mL^{-1}. The microplankton community was classified into A, B, and C1-C4 groups at a 48.1% similarity level. Groups A and B, dominated by dinoflagellates, occurred at the ends of the transect's eastern and western regions, respectively. The groups C1-C4, dominated by diatoms, were seen between groups A and B in the middle of the transect. The spatial distribution of each subgroup (C1-C4) was separated from east to west. Group C1 had the highest cell density, predominated by *Pseudo-nitzschia* spp., which was seen for the two adjacent stations at 175.0-171°W. This group is considered to have arisen due to the effect of mesoscale eddies originating from the coast of the Gulf of Alaska.

Key words: Microplankton, Community structure, Diatom, Dinoflagellate, East-west differences, Subarctic Pacific

Introduction

The subarctic Pacific extends from the coastal area of Hokkaido in the west to the Gulf of Alaska in the east. This region is known as one of the worlds major high nutrient low chlorophyll ocean areas (Harrison et al., 1999). In the subarctic Pacific, the phytoplankton community is known to vary according to the region : thus, the pennate diatoms *Fragilariopsis pseudonana*, *Pseudo-nitzschia* spp., and the centric diatom *Thalassiosira* spp. are dominant in the eastern region during summer (Aizawa et al., 2005). For the same period, the pennate diatom *Neodenticula seminae* dominates with a few centric diatoms in the northern region, while the pennate diatoms *F. pseudonana, Fragilariopsis* spp., *N. seminae*, *Pseudo-nitzschia* spp., the centric diatoms *Chaetoceros* spp. (e.g., *C. atlanticus*, *C. concavicornis*, and *C. convolutes*) and *Thalassiosira* spp. (e.g., *T. oceanica*) dominate in the western region (Aizawa et al., 2005).

Concerning the hydrographic environment, the mean sea surface temperature in the Oyashio region of the western area, can be as low at 11.4°C, and the mean nutrient concentrations can be as high as 6.0 μM nitrate, 0.774 μM phosphate, and 8.4 μM silicate during summer (Hayakawa et al., 2008). For the western subtropical Pacific, the mean diatom cell density has been reported to be extremely low (<10 cells mL^{-1}) due to a limited nutrient supply induced by strong thermocline development (Aizawa et al., 2005). In the Kuroshio transitional area of the western North Pacific, the mean sea surface temperature is higher than 20°C, and the mean nutrient concentrations are very low (0.20 μM nitrate, 0.049 μM phosphate, and 1.5 μM silicate) (Hayakawa et al., 2008). In the Oyashio region, the chlorophyll *a* (chl. *a*) concentration is correlated with the cell density of the centric diatoms ($p<0.005$) but not correlated with the pennate diatom cell density (Nosaka et al., 2017). This information suggests that diatom communities and hydrographic conditions vary greatly with region within the western North Pacific.

The biomass of zooplankton, which feed on phytoplankton, is reported to be higher in the Western Gyre than in the Alaskan Gyre (Mackas and Tsuda, 1999). Predation by micro-

1) *Laboratory of Marine Biology, Graduate School of Fisheries Sciences, Hokkaido University*
(北海道大学大学院水産科学院海洋生物学分野)
2) *Department of Environmental Biology and Fisheries Science, National Taiwan Ocean University*
(国立台湾海洋大学環境生物学・水産科学科)
3) *Laboratory of Marine Biology, Faculty of Fisheries Sciences, Hokkaido University*
(北海道大学大学院水産科学研究院海洋生物学分野)
4) *Arctic Research Center, Hokkaido University*
(北海道大学北極センター)
* Present address: Fisheries Agency
(現所属：水産庁)

zooplankton controls the standing stocks of phytoplankton in most areas of the subarctic Pacific, except for the Oyashio region (Taniguchi, 1999). Thus, east-west differences are present for zooplankton standing stocks in the subarctic Pacific, which is considered to reflect the differences in microplankton stocks and communities (Mackas and Tsuda, 1999). Despite their importance, few studies have been conducted on the east-west differences in the microplankton communities of the subarctic Pacific, and details remain unclear.

As mentioned above, studies on the phytoplankton communities in the subarctic Pacific have reported on regional changes in diatom communities (Aizawa et al., 2005), horizontal changes in chl. *a* (Hayakawa et al., 2008), and on the relationships between diatom cell density and chl. *a* (Nosaka et al., 2017). However, information on the microplankton communities of dinoflagellates and ciliates, as well as on east-west comparisons including nutrient concentration data is scarce.

For the Oyashio region in the western subarctic Pacific, a red tide composed of the harmful dinoflagellate *Karenia selliformis* was reported during the autumn of 2021 (Hasegawa et al., 2022 ; Iwataki et al., 2022 ; Takagi et al., 2022 ; Yamaguchi et al., 2022). From this point of view, microplankton communities, including dinoflagellates, are considered scientifically important. The formation of mesoscale eddies, separated from the coastal areas of the subarctic Pacific, has also been reported (Crawford et al., 2007). The effect of these mesoscale eddies on the microplankton communities of the subarctic Pacific is also an important scientific issue in need of clarification.

Bearing these backgrounds in mind, this study aimed to clarify the microplankton communities along the east-west transect of 47°N latitude in the subarctic Pacific during the summer of 2021. As a new finding from this study, the community structure analysis including dinoflagellates and ciliates, and also the east-west comparison including the nutrient data, is argued. For the analysis of the east-west differences in the microplankton communities, we applied distance-based linear modelling (DistLM) and distance-based redundancy analysis (dbRDA) to clarify the effects of environmental factors.

Materials and methods

Field sampling

The 1-L seawater samples were collected using Niskin bottles at the depth showing maximum fluorescence as detected by a fluorometer mounted on a CTD (SBE9plus) at 28 stations along the east-west transect of 47°N latitude (145.5°E-151.4°W) in the subarctic Pacific through the MR21-04 cruise of R/V *Mirai* of the Japan Agency for Marine-Earth Science and Technology (JAMSTEC) during 15 July to 13 August 2021 (Fig. 1). The sampling depths showing maximum fluorescence and their chl. *a* at each station are shown in Table 1. The sampling depths showing maximum fluorescence varied between 5.7 m and 61.5 m (Table 1). The water samples were preserved with glutaraldehyde at a final concentration of 1%. Temperature and salinity were measured using CTD at all stations. For a total of 13 stations covering a wide area from east to west, the nutrients (nitrate, nitrite, silicate, and phosphate) and chl. *a* were measured based on water samples collected at each depth using Rosette-mounted Niskin bottles on the CTD. These nutrient and chl. *a* measurements were made by JAMSTEC. The data have been published on the Data and Sample Research System for Whole Cruise Information (DARWIN) (https://www.godac.jamstec.go.jp/darwin_tmp/explain/81/j/).

Identification and enumeration

In a land-based laboratory, the 1-L preserved phytoplank-

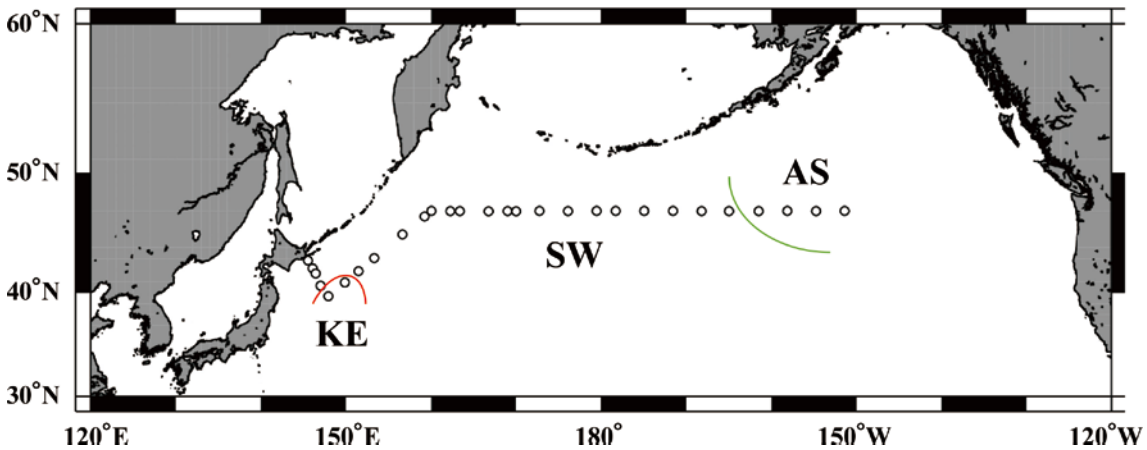

Fig. 1. Sampling location at 28 stations along the longitudinal transect mainly on 47°N in the subarctic Pacific during 15 July to 13 August 2021. Approximate positions of the boundaries between water masses (Kuroshio Extension : KE, Subarctic Water : SW, Alaskan Stream : AS, cf. Fig. 3) are indicated by the curved lines.

Table 1. Data from the water samples collected along the longitudinal transect mainly on 47°N in the subarctic Pacific during 15 July to 13 August 2021. Based on fluorescence sensor data, water samples were collected from the fluorescence maximum depth (sampling depth). For several stations, chlorophyll *a* (Chl. *a*) and nutrients were measured based on the water sampling at each depth by using rosette-mounted Niskin bottles on the CTD. The stations showing "–" have no data on Chl. *a* or nutrients because water sampling was not conducted there, although water temperature and salinity data were obtained by CTD.

Date	Latitude (°N)	Longitude	Sampling depth (m)	Chl. *a* (μg L^{-1})
15 July 2021	42.85	145.54°E	14.5	0.72
16 July 2021	42.18	146.09°E	11.1	1.80
17 July 2021	42.72	146.44°E	18.0	–
18 July 2021	40.61	147.01°E	13.3	1.27
19 July 2021	39.71	147.94°E	31.2	–
20 July 2021	40.92	149.86°E	27.2	–
21 July2021	41.94	151.49°E	29.9	–
22 July 2021	43.09	153.33°E	20.4	–
23 July 2021	45.07	156.64°E	20.1	0.88
24 July 2021	46.56	159.22°E	25.3	–
25 July 2021	47.01	160.02°E	28.1	0.76
26 July 2021	46.98	162.24°E	37.3	0.77
27 July 2021	46.99	163.39°E	33.9	–
28 July 2021	46.97	166.76°E	23.8	0.58
29 July 2021	46.99	169.00°E	30.0	–
30 July 2021	46.98	170.00°E	22.5	1.11
31 July 2021	47.00	172.72°E	25.0	–
1 Aug. 2021	47.00	176.09°E	16.8	0.75
2 Aug. 2021	47.01	179.44°E	21.3	–
3 Aug. 2021	47.00	178.31°W	50.5	–
4 Aug. 2021	47.00	174.96°W	22.4	0.57
5 Aug. 2021	47.01	171.56°W	5.7	–
6 Aug. 2021	47.00	168.20°W	10.2	0.63
7 Aug. 2021	46.99	164.99°W	5.8	–
8 Aug. 2021	47.00	161.48°W	21.2	–
13 Aug. 2021	47.00	158.14°W	6.9	0.89
12 Aug. 2021	46.99	154.75°W	26.2	–
11 Aug. 2021	47.00	151.40°W	61.5	0.28

ton samples were settled and concentrated into 20 mL samples using siphon tubes. For subsampling (usually 500 μL) of these concentrated samples, the species or genus identification and counting of microplankton cells were performed under an inverted microscope. For identification, we referred to Hasle and Syvertsen (1997) and Horner (2002) for diatoms, Steidinger and Tangen (1997) and Fukuyo et al. (1997) for dinoflagellates, and Throndsen (1997) for silicoflagellates, cryptophytes, and prasinophytes. For ciliates, identification and enumeration were made with oligotrich and tintinnid ciliates. Counting was done on approximately 300 cells for each sample. Then, the counted data were expressed with the cell density (cells mL^{-1}) of each taxon.

Data analysis

The cell density data of each taxon were standardized by the fourth root and a similarity matrix was calculated by the Bray-Curtis similarity index, then connected by the unweighted pair group method using the arithmetic mean (UPGMA) to create a dendrogram. Based on the dendrogram, the data were classified into several groups from separation at a certain similarity. In addition, one-way ANOVA was used to test microplankton cell number differences between each community, and a post hoc Tukey-Kramer test was also performed. To clarify the relationship between environmental factors and phytoplankton communities, we performed DistLM and dbRDA at 13 stations where all environmental data such as temperature, salinity, nutrients : NO_3+NO_2, phosphate, and silicate, and their ratio N : P, and Si : P were available. These cluster analyses, DistLM, and dbRDA were conducted using PRIMER 7.

Results

Hydrography

Water temperature at 0-100 m water column ranged between 1.9 and 17.3°C ; the highest temperature was found at 9.8 m at 151.5°E, and the lowest temperature was seen at 100 m at 160.0°E (Fig. 2a). Salinity values at 0-100 m depths ranged between 32.4-34.4 (Fig. 2b). The highest salinity was observed near Hokkaido Island where the observation line was meandering south to the west of 155°E. The lowest salinity was seen at shallower than 50 m to the east of 160°W near the eastern end of the line (Fig. 2b). The σT, indicating seawater density, ranged from 23.9 to 26.6. A clear pycnocline was seen around 30 m to the west of 180° (Fig. 2c). For the eastern region, low-density sea water showed an extended distribution to around 80 m, and the depth of the maximum fluorescence also became deeper in these regions.

The nutrients, including nitrogen, phosphorus, and silicates, showed similar vertical cross-section distributions to each other. Thus, low values were seen in the cases above 20 m near Hokkaido Island, while high values were seen in the depths around 50-100 m from 150°E to 180° (Fig. 2d, e, f). The N : P and Si : P (in mole ratio) showed low values above 20 m near Hokkaido Island (Fig. 2g, h). To the east of 160°W at the eastern end of the observation line, the low N : P ratio extended deep down to 80 m. The chl. *a* ranged from 0.1 to 0.8 μg L^{-1} and showed high values at 10-30 m depths near Hokkaido Island (Fig. 2i), while chl. *a* was low throughout the layers at the eastern end of the observation

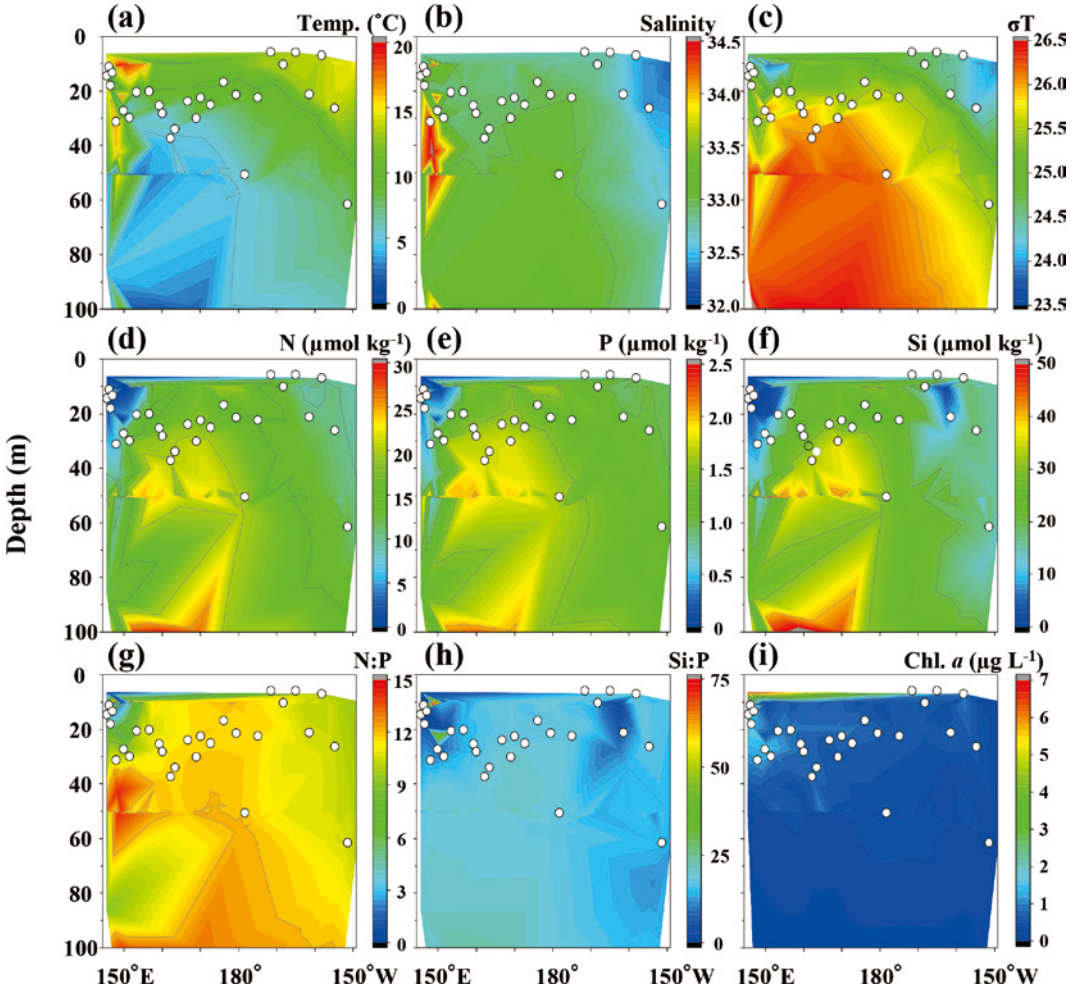

Fig. 2. Hydrography : temperature (a), salinity (b) density (σT) (c), nutrients : dissolved inorganic nitrogen (N : NO_3+NO_2) (d), PO_4 (P) (e), SiO_4 (Si) (f), nutrient ratio : N : P (g) and Si : P (h), and chlorophyll *a* (i) at the vertical section (0–100 m) of the longitudinal transect mainly on 47°N in the subarctic Pacific during 15 July to 13 August 2021 (cf. Fig. 1). The open circle symbols denote sampling depths at the fluorescence maximum.

line.

The T–S diagram based on the water temperature and salinity observed in this study is shown in Fig. 3. Based on the T–S plot area of the sea surface layer, stations could be divided into three water masses. Thus, the Alaskan stream (AS), characterized by the lowest salinity, was seen in the eastern area, the subarctic water (SW) was widely seen in the center of the east–west transect, and the Kuroshio extension (KE), having the highest salinity, was seen in the southernmost stations at the western end of the east–west transect (Fig. 1).

Microplankton community

The microplankton cell density at each station ranged from 2.3 to 117.8 cells mL^{-1} (Fig. 4a) with diatoms and dinoflagellates making up the highest proportions. Thus, diatoms accounted for 4.0–97.7% (mean : 78.3%), dinoflagellates composed 0.6–94.1% (mean : 16.6%), and ciliates shared 0.8–32.8% (mean : 3.0%).

Microplankton species and genus composition is shown in Fig. 4b. For diatoms, *Thalassiosira* spp. made up the highest proportion of centric diatoms, and *Neodenticula seminae* and *Pseudo-nitzschia* spp. the highest proportion of pennate diatoms. For dinoflagellates, *Prorocentrum* spp. made up the highest proportion, and for ciliates, naked ciliates were dominant. For the other taxa, a high proportion of the cryptomonad *Leucocryptos marina* was seen at one station (156.6°E).

The microplankton community was then classified into three groups : A, B, and C, at a 48.1% similarity level, including one outgroup station (Fig. 5a). The groups A and B were found at three and six stations, respectively, while group C occurred at 18 stations. To classify such a large group, group C was further divided into four subgroups (C1–C4) based on the dendrogram. The mean cell density and species or genus composition of each group are shown in Fig. 5b. Groups A and B were dominated by dinoflagellates, and highest and lowest cell densities were characterized by

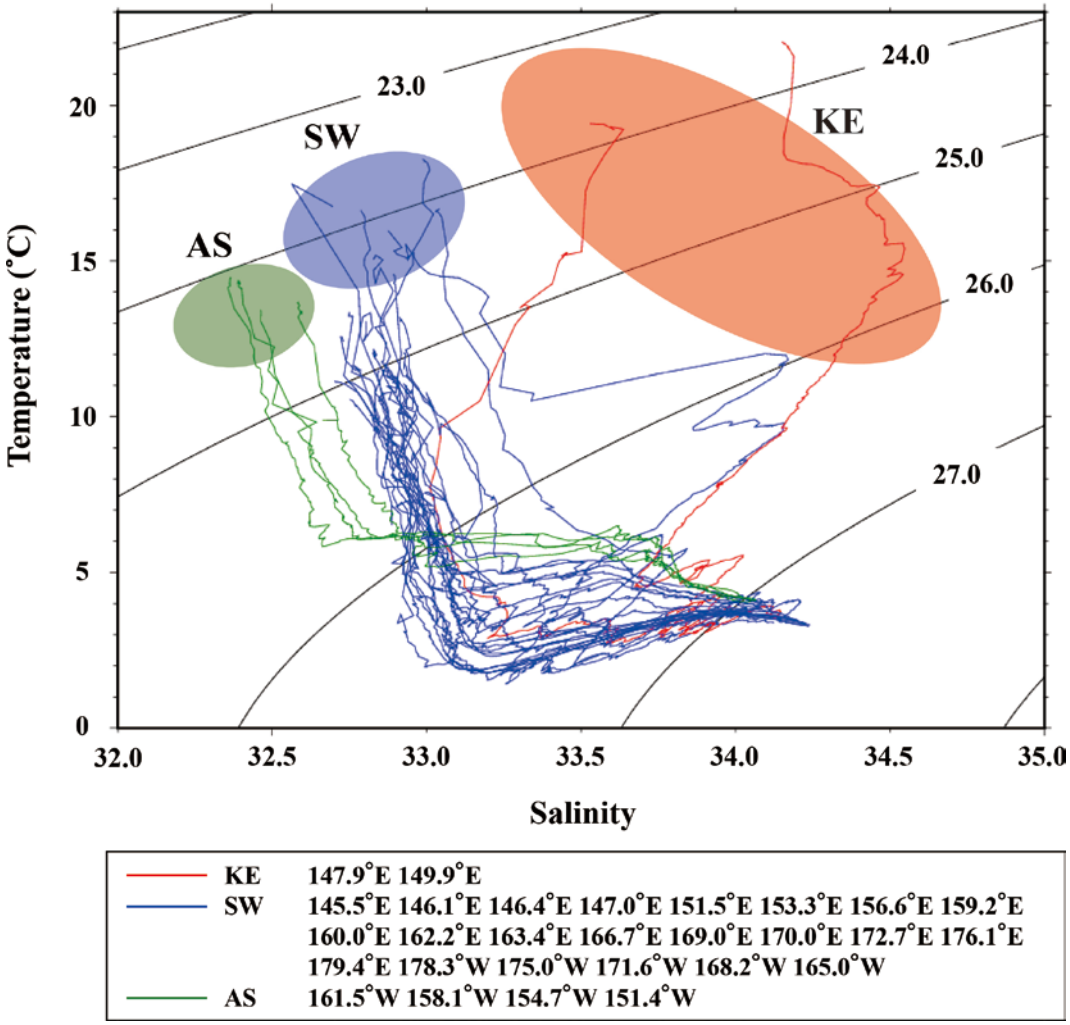

Fig. 3. T-S diagrams at each sampling station along the longitudinal transect mainly on 47°N in the subarctic Pacific during 15 July to 13 August 2021 (cf. Fig. 1). Water masses were identified based on the criteria of Anma et al. (1990). AS : Alaskan Stream, SW : Subarctic Water, KE : Kuroshio Extension.

groups A and B, respectively. Group C1 had the highest cell density and was predominated by *Pseudo-nitzschia* spp. Groups C2 to C4 were dominated by diatoms showing middle cell densities. Group C2 had a high proportion of *Thalassiosira* spp., group C4 had a high proportion of *Neodenticula seminae*, and group C3 was dominated by other centric diatoms.

The mean cell density of each microplankton genus and species in each group is shown in Table 2. Within the 49 genera/species treated in this study, significant inter-group differences in cell density were seen in twelve genera/species. For genus/species showing significant inter-group differences in cell density, most genus/species showed high densities in groups A or C1. On the other hand, several species, *Actinocyclus ingens* and *Bellerochea heptactis,* had high cell densities in group C3. It also should be noted that the dominant diatom species, *Chaetoceros* spp., *Leptocylindrus mediterraneus*, *Neodenticula seminae*, and *Peudo-nitzschia* spp. in group C1 showed their lowest abundances in group A.

In the dbRDA diagram, dbRDA1 explained 29.0% of the total variation, and dbRDA2 explained 16.9% (Fig. 5c). All analyzed environmental data had significant directions in the dbRDA plot. One outgroup station (151.4°W) was plotted for low temperature, salinity, and nutrients. Notably, the directions of two nutrient ratios, Si : P and N : P, were opposed in the dbRDA plot. Group A was distributed in the direction characterized by the high Si : P ratio.

East-west differences

The east-west distribution of environmental factors (temperature, salinity, water masses, nutrients, and nutrient ratios) and microplankton communities (each group and the cell densities of diatoms and dinoflagellates) in this study are shown in Fig. 6. The groups A and B, dominated by dinoflagellates, were only observed at both the eastern and western ends of the observation line. Group A, characterized by high cell density, was only seen near Hokkaido Island at the western end of the observation line. The cell density of dinoflagel-

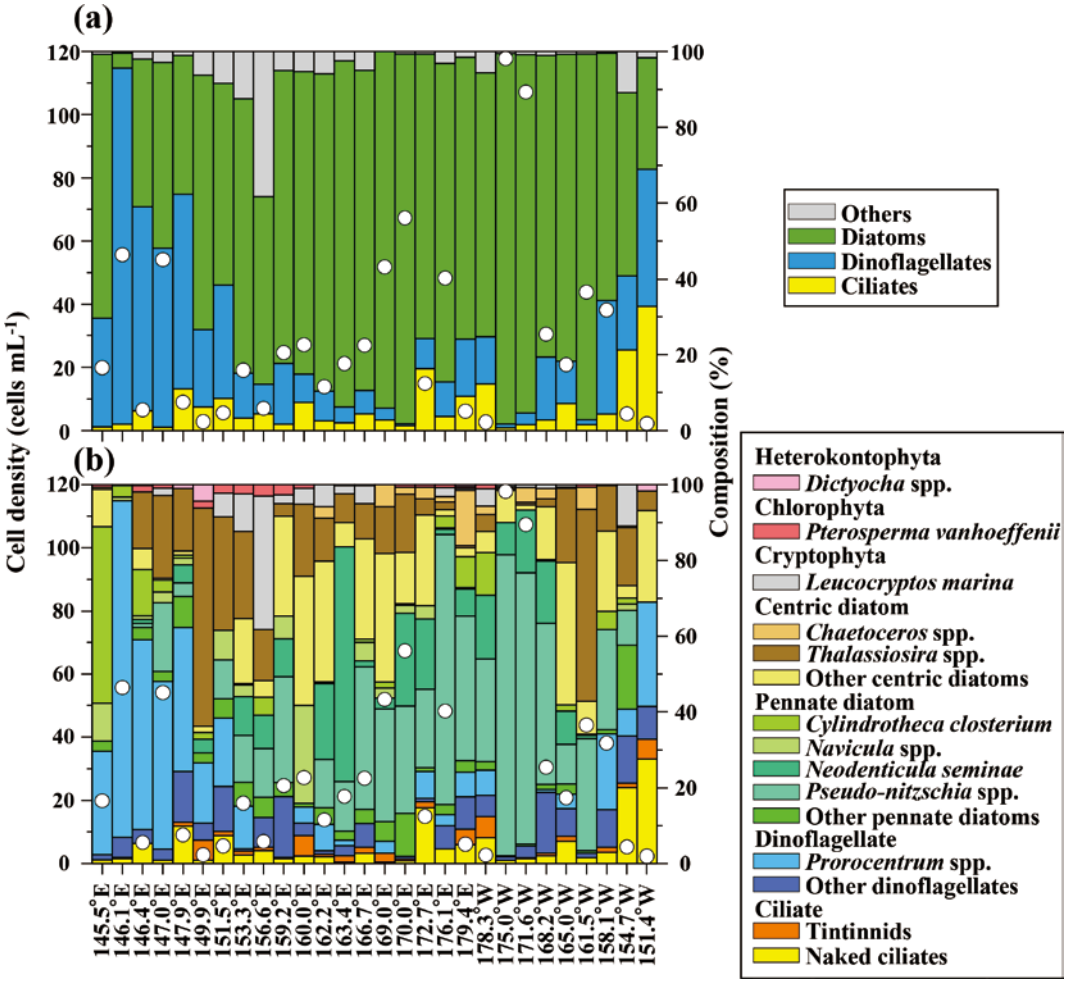

Fig. 4. Cell density and taxonomic composition of microplankton at fluorescence maximum layer of 28 stations along the longitudinal transect mainly on 47°N in the subarctic Pacific during 15 July to 13 August 2021. For the taxonomic accounts, the large deviations are shown in (a) and the species compositions are shown in (b).

lates was highest at the western end of the observation line, which also showed the lowest nutrient concentrations and highest Si : P and N : P ratios.

Group C, characterized by the dominance of the diatoms, was seen in the middle of the observation line (Fig. 6). For the subgroups of group C, east-west differences in their distribution were present. Thus, group C3 was seen in the western region (154-170°E), and group C4 was seen in the eastern region (162°E-176°W). Group C1, characterized by the highest cell density, occurred at 170°E-175°W, coinciding with an area of high water temperature and low salinity. Further east, group C2 distributed widely between 156°E-175°W.

Discussion

Microplankton community

In this study, the microplankton community in the summer subarctic Pacific was classified into six groups : A, B, and C1-C4 (Fig. 5). We will now discuss the characteristics of each community. For group A, the dominant dinoflagellate *Prorocentrum* spp. was most dominant at St. KNOT (44°N, 155°E) in the western subarctic Pacific in August, where the sea surface temperature and salinity were 14°C and 32.8, respectively (Mochizuki et al. 2002). These hydrographic conditions are very consistent with the other marine environments where group A was seen (Fig. 2). With regard to nutrients, the concentrations of N, P, and Si at St. KNOT in August have been reported as <10 μmol kg^{-1}, <1 μmol kg^{-1}, and <10 μmol kg^{-1}, respectively (Mochizuki et al. 2002). These nutrient concentrations are also consistent with the values observed for group A in this study (Fig. 6). With water mass, group A was seen to a transition area between KE and SW. This area was characterized by high sea surface temperatures and almost depleted nutrient levels lower than to the east of 170°W. These water mass characteristics are well consistent with the previously reported conditions for this area in summer (Hayakawa et al., 2008). These facts suggest that *Prorocentrum* spp. can dominate under warm, low salinity, low nutrient oligotrophic conditions.

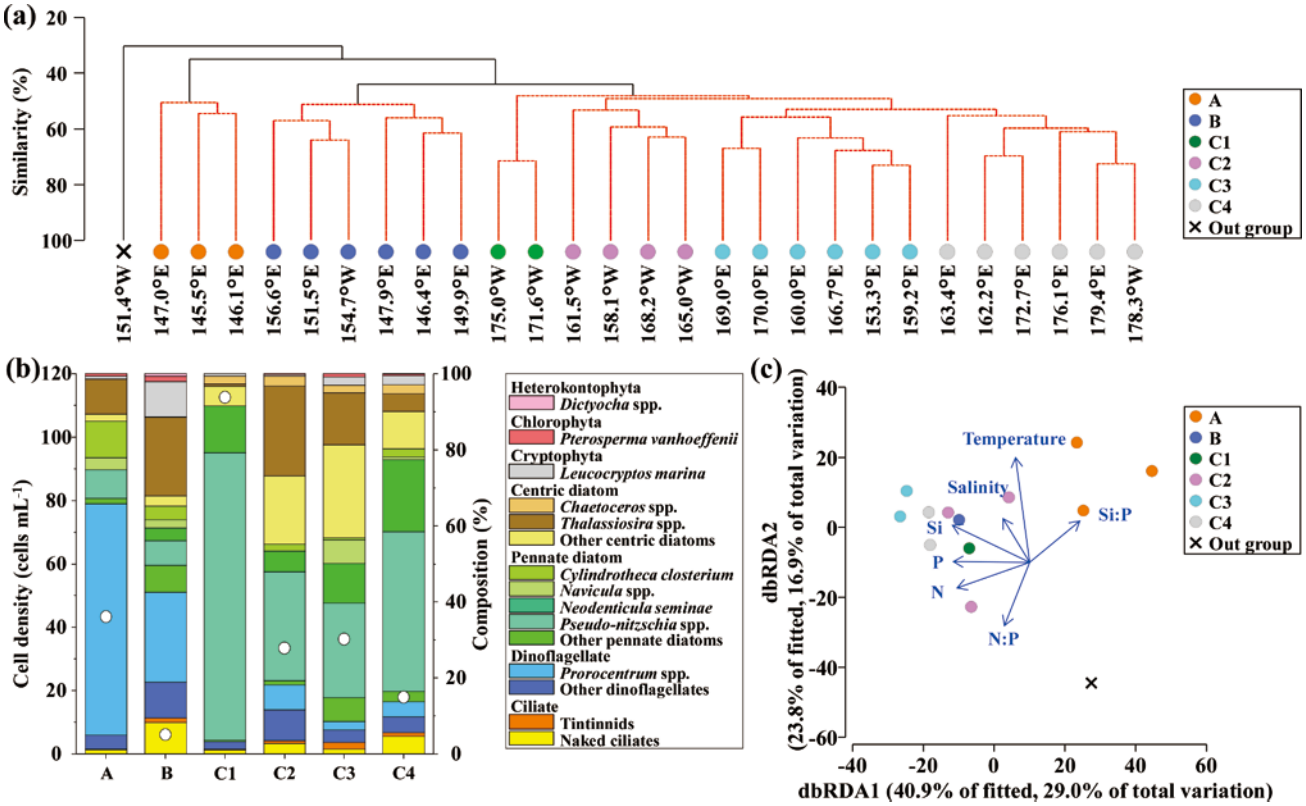

Fig. 5. Results of cluster analysis from Bray-Curtis similarity based on cell density data standardized by fourth-root at each station along the longitudinal transect mainly on 47°N in the subarctic Pacific during 15 July to 13 August 2021 (a). Six groups, including four sub-groups (A, B, C1, C2, C3, C4), were identified. Mean cell density and their taxonomic composition are shown in (b). dbRDA plots of six groups including four sub-groups (A, B, C1, C2, C3, C4) identified by the cluster analysis based on the cell density with environmental parameters (temperature, salinity, N, Si, N : P, and Si : P) (c). The arrowhead direction and length of the arrow lines in the middle of the panel indicate the relationships between groups and the strength of the parameters. Note that the data used for dbRDA were derived only from the thirteen stations having nutrient data (cf. Table 1).

Like group A, group B was also dominated by dinoflagellates, but its cell density was lower than that of group A (Fig. 5b). Considering the hydrographic conditions of group B, the salinity was similar, but the water temperature (5 to 7.5°C) was lower than that of group A (Fig. 6). According to Mochizuki et al. (2002), warm water temperature conditions are necessary for the cell division of dinoflagellates. Thus, the slightly cold condition of group B may induce the low cell density of dinoflagellates compared with group A.

Group C1 was characterized by diatoms (Fig. 5b). The wide distribution of *Pseudo-nitzschia* spp. from the coastal area along Japan, subarctic and subtropical areas in both eastern and western Pacific, and the Bering Sea has previously been reported (Aizawa et al. 2005). While *Pseudo-nitzschia* spp. have been reported to distribute across a wide geographical range throughout the North Pacific, the extremely high density found in this study was not reported by Aizawa et al. (2005). Sympatrically in the North Pacific, the occurrence of the dinoflagellate *Gyrodinium* spp., which can consume large-sized diatoms such as the chain-forming *Chaetoceros* spp. and *Pseudo-nitzschia* spp., which are larger than their cell length, has been reported (Saito et al., 2006). However, *Gyrodinium* spp. did not occur in the same area as group C1 in this study (Table 2).

For groups C2-C3, the diatom *Thalasiosira* spp., which characterizes group C2 (Fig. 5b), has been reported to be widely distributed throughout the western and eastern subarctic Pacific and the Bering Sea areas (Aizawa et al., 2005). It has also been pointed out that the regions dominated by *Thalassiosira* spp. were co-dominated by the centric diatom *Chaetoceros* spp. (Aizawa et al., 2005). The co-dominance of *Thalassiosira* spp. and *Chaetoceros* spp. has also been seen for group C, while *Chaetoceros* spp. was not recorded in the cases of groups A and B (Fig. 5).

Group C4 was dominated by *N. seminae* in the center of the east-west observation line of this study (Fig. 5b). The high cell density of *N. seminae* at 49.3°N and 172.5°E has been reported by Aizawa et al. (2005). Reporting on the hydrographic characteristics responsible for the dominance of *N. seminae*, Aizawa et al. (2005) reported that the sea surface temperature and salinity were 9.2°C and 32.4, respec-

Table 2. Mean microplankton cell density at six groups identified from cluster analysis (cf. Fig. 5a). Numbers in parentheses indicate the number of samples included in each group. Differences between groups were tested by one-way ANOVA and Tukey-Kramer tests. Any groups not connected by underlines were significantly different ($p < 0.05$). NS : not significant * : $p < 0.05$; ** : $p < 0.01$; *** : $p < 0.001$.

Taxa/species	Group						one-way ANOVA	Tukey-Kramer test
	A (3)	B (6)	C1 (2)	C2 (4)	C3 (6)	C4 (6)		
Heterokontophyta								
Dictyocha spp.	0	0.04	0	0	0	0.02	NS	
Chlorophyta								
Pterosperma vanhoeffenii	0.26	0.08	0	0.10	0.31	0.08	NS	
Cryptophyta								
Leucocryptos marina	0.36	0.56	0.72	0.11	0.81	0.43	NS	
Centric diatom								
Actinocyclus ingens	0	0	0.44	0	1.29	0.44	**	A B C2 C1 C4 C3
Asteromphalus heptactis	0	0.07	0.29	2.34	0.13	0.06	NS	
Bellerochea horologicalis	0	0	0	3.27	6.32	0.90	*	B A C1 C4 C2 C3
Chaetoceros aequatorialis	0	0	0	0	0	0.16	NS	
Chaetoceros atlanticus	0	0	0	0.75	0.21	0.01	NS	
Chaetoceros concavicornis	0	0	1.27	0.12	0.10	0.14	***	A B C3 C2 C4 C1
Chaetoceros danicus	0	0	1.11	0	0	0	*	A B C2 C3 C4 C1
Chaetoceros lorenzianus	0	0	0	0	0.41	0.10	NS	
Corethron criophilum	0	0.02	0.42	0	0.13	0.21	NS	
Dactyliosolen fragilissimus	0.66	0	0	0	0	0	*	C3 C4 B C1 C2 A
Guinardia striata	0.09	0.01	0	0	0	0	NS	
Leptocylindrus danicus	0	0	0	0	0.06	0	NS	
Leptocylindrus mediterraneus	0	0	4.09	0	0.16	0	*	A B C2 C4 C3 C1
Odontella aurita	0	0.01	0	0	0.09	0.02	NS	
Proboscia alata	0	0	0	0.17	0.61	0.08	NS	
Skeletonema costatum	0	0	0.45	0.21	0	0	NS	
Thalassionema nitzschioides	0.13	0.02	0	0	0.92	0	NS	
Thalassiosira delicatula	0	0.03	0	6.31	0	0	NS	
Thalassiosira eccentrica	0	0.03	0.14	0.18	0.59	0.17	NS	
Thalassiosira pacifica	3.97	1.18	0.58	1.36	4.35	0.65	NS	
Other centric diatoms	0	0.06	0	0	0.04	0.05	NS	
Pennate diatom								
Amphora spp.	0	0.04	0	0.17	0.45	0.06	NS	
Bacillaria spp.	0.10	0	0	0	0	0	NS	
Cylindrotheca closterium	4.20	0.22	0	0.62	0.22	0.39	*	C1 B C3 C4 C2 A
Fragilariopsis doloulus	0	0.01	0	0	0	0	NS	
Fragilariopsis kergulensis	0	0.02	0	0	0	0	NS	
Haslea spp.	0.04	0.26	0	0.07	0.31	0.05	NS	
Navicula spp.	1.37	0.12	0	0	2.22	0.13	*	Not detected
Neodenticula seminae	0	0.20	13.86	1.81	3.80	3.36	*	A B C2 C4 C3 C1
Nitzschia spp.	0	0.04	0	0	0.13	0.25	NS	
Pseudo-nitzschia spp.	3.26	0.39	85.15	9.55	8.98	7.51	***	B A C4 C3 C2 C1
Thalassiothrix longissima	0.05	0	0.43	0.09	0.41	0.04	NS	
Tropidoneis antarctica	0	0	0	0	0.04	0	NS	
Other pennate diatoms	0.31	0.04	0	0.09	0.04	0.06	NS	
Dinoflagellate								
Amphidinium spp.	0.10	0.01	0	0	0	0	NS	
Ceratium spp.	0.42	0.03	0	0.23	0.01	0	NS	
Dinophysis spp.	0	0	0	0.05	0	0	NS	
Gymnodinium spp.	0	0.10	0.98	1.67	0.32	0.24	NS	
Heterocapsa spp.	0	0.12	0.55	0.27	0.68	0	NS	
Katodinium spp.	0	0.01	0.58	0.12	0	0.29	NS	
Prorocentrum spp.	26.30	1.42	0	2.18	0.81	0.70	**	C1 C4 C3 B C2 A
Protoperidinium spp.	0.15	0.11	0.15	0.30	0.13	0.06	NS	
Pyrophacus spp.	0.76	0.01	0	0	0	0	*	C2 C3 C4 B C1 A
Scrippsiella spp.	0.16	0.18	0	0.03	0.04	0.16	NS	
Ciliate								
Tintinnids	0.06	0.07	0.14	0.25	0.65	0.18	NS	
Naked ciliates	0.46	0.49	1.15	0.92	0.43	0.80	NS	
Total	43.21	6.00	112.50	33.32	36.18	17.80	***	B C4 C2 C3 A C1

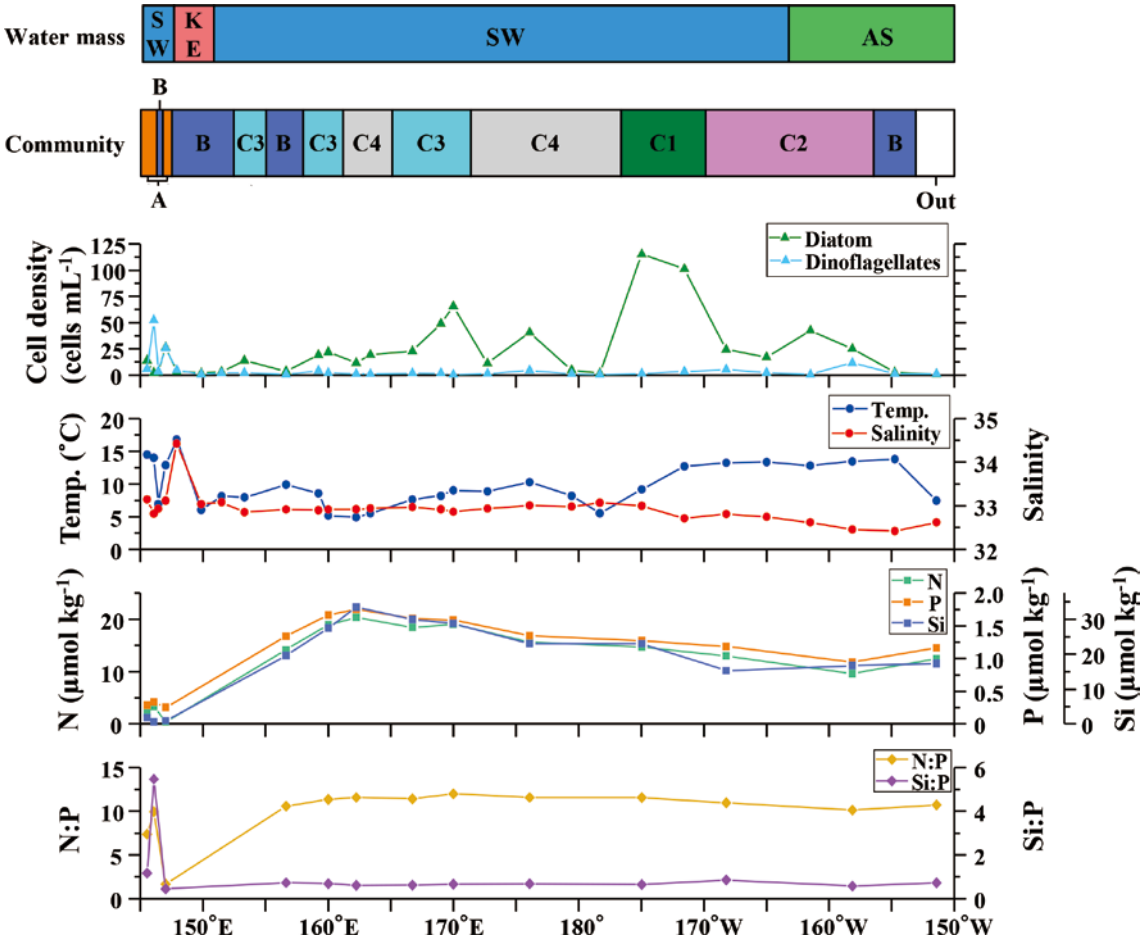

Fig. 6. East-west differences in microplankton community and environmental parameters along the longitudinal transect mainly on 47°N in the subarctic Pacific during 15 July to 13 August 2021. From upper to lower, the panels are on : water masses (SW : subarctic water, KE : Kuroshio extension, AS : Alaskan stream), microplankton community (A, B, C1, C2, C3, C4), cell density of diatom and dinoflagellates, temperature and salinity, nutrients : NO_2+NO_3 (N), PO_4 (P), SiO_4 (Si), and nutrient ratio : N : P, Si : P in mole.

tively. In the present study, the hydrographic characteristics of group C4 displayed lower temperatures than those of Aizawa et al. (2005) (Fig. 6).

Overall, high cell densities occurred in the cases of groups A and C1. However, the dominant species varied greatly between groups A and C1 (Table 2). The water temperature and salinity of these two groups were almost identical ; the only difference was seen in the nutrient concentrations. Thus, group A was characterized by low nutrient concentrations and low N : P ratio (Fig. 6). Concerning N : P and Si : P ratios, phosphate limitations have been reported to occur at N : P>22 and Si : P>2 (Wang et al., 2021). In this study, ocean areas where Si : P ratios exceeded two were seen near Hokkaido Island, suggesting that a limitation of phosphate may be occurring there (Fig. 6). These areas (Si : P>2) coincided with the area where group A was observed (Fig. 6). These facts suggest that while water temperature and salinity were similar, the nutrient concentrations and their ratios may be responsible for the difference in the species composition of the microplankton communities in both areas. The differences in dominant species in sea areas are derived from inter-species differences in development, growth, and survival strategies of microplankton species/taxa on each nutrient concentration.

East-west differences

Considering the east-west differences in microplankton communities, within the groups A and B dominated by dinoflagellates, group A, characterized by high cell density, occurred near Hokkaido Island at the western end of the observation line (Fig. 6). This region is where a marine heat wave was observed from mid-July to mid-August 2021 (Kuroda and Setou, 2021 ; Kuroda et al., 2021). A possible explanation for the dominance of dinoflagellates in this area, could be that as the marine heat wave thermocline develops, and nutrients become depleted at the surface layer, the normal phytoplankton taxa which having no swimming ability (e.g., diatoms) cannot grow, whereas dinoflagellates which can swim by using their flagella can replenish nutrients by migrating down to deeper layer at night, thereby achieve dominance

in microplankton community (Yamaguchi et al., 2022). These mechanisms may explain the massive red tide of the harmful dinoflagellate *K. selliformis*, which performs diel vertical migration, that occurred in this area during the fall of 2021 (Hasegawa et al., 2022 ; Iwataki et al., 2022 ; Takagi et al., 2022 ; Yamaguchi et al., 2022). Group A, which was dominated by dinoflagellates under warm and nutrient-depleted conditions, is thought to be a reflection of this situation.

Group B was seen slightly off both ends of the east-west observation line, which correspond to the low-salinity waters originating from the Hokkaido coast and the Gulf of Alaska coast, respectively (Fig. 6). The occurrence of the low-density dinoflagellate communities in these areas is thought to be a reflection of the water masses which have become nutrient-depleted after the spring phytoplankton bloom. In the present study, the N : P and Si : P ratios were highly fluctuating near Hokkaido Island (Fig. 6). This is thought to be an artifact caused by deficient concentrations of three nutrients N, P, and Si after the spring phytoplankton bloom in the adjacent coastal waters (Fig. 2d, e, f).

In group C1, the diatom *Pseudo-nitzschia* spp. was predominant at two horizontally adjacent stations (175.0-171.6°W). The water temperature and salinity at these stations were higher and lower, respectively than those to the west of 175°W (Fig. 6). Since the salinity at these two stations was substantially lower than the other adjacent stations, it is thought that low salinity water had been transported from the coastal area due to the action of the mesoscale eddies. There is a counterclockwise circulation termed the Alaskan Gyre in the Gulf of Alaska, which ultimately flows along the Aleutian Islands into the central subarctic Pacific as the Alaskan Stream (Crawford et al., 2007). It has been reported that multiple mesoscale eddies form off the coast of the Gulf of Alaska in winter, separate from the continental shelf in late winter to spring, then remain in the subarctic Pacific until late summer (Crawford et al., 2007). One function of these mesoscale eddies is to transport iron-rich coastal water to the iron-limited oceanic regions, providing sufficient conditions for phytoplankton growth through mixing (Crawford et al., 2005). Based on shipboard experiments, the growth of the diatom *Pseudo-nitzschia* spp. is accelerated under incubation using a mixture of mesoscale eddy water and oceanic water as the incubation water (Peterson et al., 2011). These facts indicate that the phytoplankton bloom is achieved by using iron which is supplied to the subarctic Pacific by the mesoscale eddies separated from the Gulf of Alaska coast. As the result of the bloom, it can be interpreted that the cell densities of pennate diatoms at these two stations points showed the highest values among the observation line.

Acknowledgments

The phytoplankton samples and hydrographic data used in this study were collected from JAMSTEC's R/V *Mirai*. We sincerely thank Dr. Shinya Kouketsu, the cruise's chief scientist, the captain, the crew, and scientists onboard during the cruise for their great help in collecting samples and obtaining the hydrographic data used in this study. We also thank the Special Research Student Program between National Taiwan University and Hokkaido University for allowing us to make the international academic exchange. This study was partially supported by a Grant-in-Aid for Challenging Research (Pioneering) 20K20573, Scientific Research 22H00374 (A), 20H03054 (B), 19H03037 (B), and 17H01483 (A) from the Japan Society for the Promotion of Science (JSPS). It was also partially supported by the Arctic Challenge for Sustainability II (ArCS II ; JPMXD1420318865) and the Environmental Research and Technology Development Fund (JPMEERF20214002) of the Environmental Restoration and Conservation Agency of Japan.

References

Aizawa, C., Tanimoto, M. and Jordan, R.W. (2005) Living diatom assemblages from North Pacific and Bering Sea surface waters during summer 1999. *Deep-Sea Res II*, **52**, 2186-2205.

Anma, G., Masuda, K., Kobayashi, G., Yamaguchi, H., Meguro, T., Sasaki, S. and Ohtani, K. (1990) Oceanographic structures and changes around the transition domain along 180 degree longitude, during June 1979-1988. *Bull. Fac. Fish. Hokkaido Univ.*, **41**, 73-88.

Crawford, W.R., Brickley P.J. and Thomas A.C. (2007) Mesoscale eddies dominate surface phytoplankton in northern Gulf of Alaska. *Prog. Oceanogr.*, **75**, 287-303.

Crawford, W.R., Brickley, P.J., Peterson, T.D. and Thomas, A.C. (2005) Impact of Haida Eddies on chlorophyll distribution in the eastern Gulf of Alaska. *Deep-Sea Res. II*, **52**, 975-989.

Fukuyo, Y., Inoue, H. and Takayama, H. (1997) Class Dinophyceae. pp. 31-112, Chihara, M. and Murano, M. (eds), *An Illustrated Guide to Marine Plankton in Japan*. Tokai University Press, Tokyo.

Harrison, P.J., Boyd, P.W., Varela, D.E., Takeda, S., Shiomoto, A. and Odate, T. (1999) Comparison of factors controlling phytoplankton productivity in the NE and NW subarctic Pacific gyres. *Prog. Oceanogr.*, **43**, 205-234.

Hasegawa, N., Watanabe, T., Unuma, T., Yokota, T., Izumida, D., Nakagawa, T., Kurokawa, T., Takagi, S., Azumaya, T., Taniuchi, Y., Kuroda, H., Kitatsuji, S. and Abe, K. (2022) Repeated reaching of the harmful algal bloom of *Karenia* spp. around the Pacific shoreline of Kushiro, eastern Hokkaido, Japan, during autumn 2021. *Fish. Sci.*, **88**, 787-803.

Hasle, G.R. and Syvertsen, E.E. (1997) Marine diatoms. pp. 5-385, Tomas, C.R. (ed.), *Identifying Marine Phytoplankton*. Academic Press, San Diego.

Hayakawa, M., Suzuki, K., Saito, H., Takahashi, K. and Ito, S. (2008) Differences in cell viabilities of phytoplankton between spring and late summer in the northwest Pacific Ocean. *J.*

Exp. Mar. Biol. Ecol., **360**, 63–70.

Horner, R.A. (2002) *A Taxonomic Guide to Some Common Marine Phytoplankton*, Biopress Limited, United Kingdom.

Iwataki, M., Lum, W.M., Kuwata, K., Takahashi, K., Arima, D., Kuribayashi, T., Kosaka, Y., Hasegawa, N., Watanabe, T., Shikata T., Isada, T., Orlova T.Y. and Sakamoto, S. (2022) Morphological variation and phylogeny of *Karenia selliformis* (Gymnodiniales, Dinophyceae) in an intensive cold-water algal bloom in eastern Hokkaido, Japan. *Harmful Algae*, **114**, 102204, doi.org/10.1016/j.hal.2022.102204.

Kuroda, H. and Setou, T. (2021) Extensive marine heatwaves at the sea surface in the northwestern Pacific Ocean in summer 2021. *Remote Sens.*, **13**, 3989, doi.org/10.3390/rs13193989.

Kuroda, H., Azumaya T., Setou. T. and Hasegawa, N. (2021) Unprecedented outbreak of harmful algae in Pacific coastal waters off southeast Hokkaido, Japan, during late summer 2021 after record-breaking marine heatwaves. *J. Mar. Sci. Eng.*, **9**, 1335, doi.org/10.3390/jmse9121335.

Mackas, D.L. and Tsuda, A. (1999) Mesozooplankton in the eastern and western subarctic Pacific : community structure, seasonal life histories, and interannual variability. *Prog. Oceanogr.*, **43**, 335–363.

Mochizuki, M., Shiga, N., Saito, M., Imai, K. and Nojiri, Y. (2002) Seasonal changes in nutrients, chlorophyll *a* and the phytoplankton assemblage of the western subarctic gyre in the Pacific Ocean. *Deep-Sea Res. II*, **49** 5421–5439.

Nosaka, Y., Yamashita, Y. and Suzuki, K. (2017) Dynamics and origin of transparent exopolymer particles in the Oyashio region of the western subarctic Pacific during the spring diatom bloom. *Front. Mar. Sci.*, **4**, 79, doi.org/10.3389/fmars.2017.00079.

Peterson, T.D., Crawford, D.W. and Harrison, P.J. (2011) Mixing and biological production at eddy margins in the eastern Gulf of Alaska. *Deep-Sea Res. II*, **58,** 377–389.

Saito, H., Ota, T., Suzuki, K., Nishioka, J. and Tsuda A. (2006) Role of heterotrophic dinoflagellate *Gyrodinium* sp. in the fate of an iron induced diatom bloom. *Geophys. Res. Lett.*, **33**, L025366, doi.org/10.1029/2005GL025366.

Steidinger, K.A. and Tangen, K. (1997) Dinoflagellates. pp. 387–584, Tomas, C.R. (ed.), *Identifying Marine Phytoplankton*. Academic Press, San Diego.

Takagi, S., Kuroda, H., Hasegawa, N., Watanabe, T., Unuma, T., Taniuchi, Y., Yokota, T., Izumida, D., Nakagawa, T., Kurokawa, T. and Azumaya, T. (2022) Controlling factors of large-scale harmful algal blooms with *Karenia selliformis* after record-breaking marine heatwaves. *Front. Mar. Sci.*, **9**, 939393, doi.org/10.3389/fmars.2022.939393.

Taniguchi, A. (1999) Differences in the structure of the lower trophic levels of pelagic ecosystems in the eastern and western subarctic Pacific. *Prog. Oceanogr.*, **43**, 289–315.

Throndsen, J. (1997) The planktonic marine flagellates. pp. 591–715, Tomas, C.R. (ed.), *Identifying Marine Phytoplankton.* Academic Press, San Diego.

Wang, Y., Kang, J., Sun, X., Huang, J., Lin, Y. and Xiang, P. (2021) Spatial patterns of phytoplankton community and biomass along the Kuroshio Extension and adjacent waters in late spring. *Mar. Biol.*, **168**, 40, doi.org/10.1007/s00227-021-03846-7.

Yamaguchi, A., Hamao, Y., Matsuno, K. and Iida, T. (2022) Horizontal distribution of harmful red-tide *Karenia selliformis* and phytoplankton community along the Pacific coast of Hokkaido in autumn 2021. *Bull. Japan. Soc. Fish. Oceanogr.*, **86**, 41–49.